# Synthesis and characterization of a cobalt(II) tetrakis(3-fluorophenyl) porphyrin with a built-in 4-vinylphenyl surface attachment moiety

D. KHUSNUTDINOVA, M. FLORES, A.M. BEILER, and G.F. MOORE<sup>+</sup>

School of Molecular Sciences and the Biodesign Institute Center for Applied Structural Discovery (CASD), Arizona State University, Tempe, AZ 85287-1604, USA

## **Abstract**

Metalloporphyrins serve important roles in biology and as components in emerging technological assemblies for energy conversion. In this report, we describe the synthesis and characterization of a novel cobalt(II) 5,10,15,20-tetrakis (3-fluorophenyl)porphyrin bearing a 4-vinylphenyl surface attachment group at a beta position on the macrocycle. Electrochemical measurements show the 3-fluorophenyl groups at the meso positions of the porphyrin perturb the reduction potentials of the complex to more positive values as compared to non-fluorinated analogs, thus allowing access to reduced cobalt porphyrin species at significantly less negative applied bias potentials. The complex, cobalt(II) 5,10,15,20-tetrakis(3-fluorophenyl)-2-(4-vinylphenyl)porphyrin, is abbreviated in this article as Gov-1 in honor of Govindjee for his pioneering investigations in the role of fluorine as a promoter of novel protein-substrate interactions and the inspirational role he continues to have in encouraging young investigators in the areas of natural and artificial photosynthesis.

Additional key words: artificial photosynthesis; fluorine; porphyrins; surface chemistry.

### Introduction

Fluorine substitution provides a powerful synthetic tool in organic and bioorganic chemistry (O'Hagan and Rzepa 1997, Chambers 2004). The chemical stability and relatively small size of fluorine coupled with its highly electron-withdrawing nature (a 4.0 on the Pauling scale) are attractive features. In addition to the use of fluoro groups as reporters in <sup>19</sup>F NMR studies (Gerig 1978, Sykes et al. 1978, Toi 1985, Dalvit and Vulpetti 2011), this highly electronegative group has shown promise in promoting novel protein-substrate as well as proteinprotein interactions (Tierno et al. 1990, Kim et al. 2000, Yolder and Kumar 2002) and provides a molecular strategy for tuning the electrochemical properties of redox catalysts and mediators (Rosenthal et al. 2006, Moore et al. 2008, 2012b, Berben and Peters 2010, Rose et al. 2012, Cedeno et al. 2014). Herein, we report the synthesis and characterization of a cobalt(II) porphyrin substituted with 3-fluorophenyl groups at all four meso positions of the porphyrin ring and a single 4-vinylphenyl surface attachment group at one of the beta positions.

Porphyrins serve important roles in living systems and as molecular components in technological assemblies for sensor applications, catalysis, and energy transduction. As an example of the latter, we have recently reported a synthetic methodology to chemically graft metalloporphyrins to visible-light-absorbing semiconductors (Khusnutdinova *et al.* 2017) for construction of an integrated photocathode with applications in artificial photosynthesis (Bard and Fox 1995, Blankenship *et al.* 2011, Najafpour *et al.* 2012, Faunce *et al.* 2013a,b; Hou *et al.* 2017, Maher *et al.* 2017, Moore 2017) including light activation of chemical transformations for capturing,

Received 30 June 2017, accepted 5 September 2017, published as online-first 15 January 2018.

<sup>\*</sup>Corresponding author; e-mail: gfmoore@asu.edu

Abbreviations: DDQ – 2,3-dichloro-5,6-dicyano-1,4-benzoquinone; EPR – electron paramagnetic resonance; Fc<sup>+</sup>/Fc – ferrocenium/ ferrocene; FTIR – Fourier transform infrared; gCOSY – gradient correlation spectroscopy; Gov-1 – cobalt(II) 5,10,15,20-tetrakis(3-fluorophenyl)-2-(4-vinylphenyl)porphyrin; m/z – abbreviation representing the dimensionless quantity formed by dividing the ratio of the mass of an ion to the unified atomic mass unit, by its charge number; MALDI-TOF MS – matrix assisted laser desorption/ ionization time-of-flight mass spectrometer; NBS – N-bromosuccinamide; NMR – nuclear magnetic resonance; SCE – standard calomel reference electrode; UV-Vis – ultraviolet-visible; 4-VPBA – 4-vinylphenyl boronic acid;  $\delta$  – chemical shift.

Acknowledgments: NMR studies were performed using the Magnetic Resonance Research Center at Arizona State University. This material is based upon work supported by the National Science Foundation under Early Career Award 1653982. A.M. Beiler was supported by an IGERT-SUN fellowship funded by the National Science Foundation (Award 1144616). D. Khusnutdinova acknowledges support from ASU LightWorks under the Technology and Research Initiative Fund.

converting, and storing solar energy in the form of chemical bonds. In this assembly, the semiconductor serves as a light capture and conversion component as well as a physical support for assembling the modified cobalt porphyrin hydrogen production catalysts. The attachment chemistry used to graft the porphyrin complex to the semiconductor surface leverages the UV-induced grafting of alkenes to hydrogen and hydroxyl terminated surfaces (Cicero et al. 2000, Li et al. 2009, Richards et al. 2010, Steenackers et al. 2011, Seifert et al. 2013, Moore and Sharp 2013, Cedeno et al. 2015, Beiler et al. 2016a,b, 2017; Wadsworth et al. 2016). Thus the assembly combines solid-state light capture and conversion materials with molecular surface coatings to enhance photoelectrochemical fuel production activity.

For the fluorinated porphyrin analog described in this report, electrochemical measurements show the  $Co^{II/I}$  redox process occurs  $\approx 100$  mV less negative than that of the previously reported nonfluorinated analog (Khusnutdinova *et al.* 2017). In addition, a second reduction process, occurring at more negative potentials and assigned to the  $Co^{I}/Co^{0}$  couple, is clearly resolved within the electro-

#### Materials and methods

All reagents and solvents were purchased from *Aldrich*. Dichloromethane, hexanes, and toluene were freshly distilled before use. Reactions were performed under argon atmosphere unless otherwise stated.

**Experimental section**: Ultraviolet-visible (UV-Vis) optical spectra were recorded on a Shimadzu SolidSpec-3700 spectrometer with a deuterium lamp for the ultraviolet range. <sup>1</sup>H, <sup>13</sup>C, and <sup>19</sup>F nuclear magnetic resonance (NMR) spectra were recorded on a Varian NMR spectrometer operating at 400 MHz at room temperature. All <sup>1</sup>H and <sup>13</sup>C NMR chemical shifts (δ) are reported relative to Si(CH<sub>3</sub>)<sub>4</sub> as an internal standard. <sup>19</sup>F data are reported relative to C<sub>6</sub>H<sub>5</sub>CF<sub>3</sub> (-63.77 ppm). Mass spectra were obtained using a Voyager DE STR matrix-assisted laser desorption/ionization time-of-flight mass spectrometer (MALDI-TOF MS) in positive ion mode with trans,trans-1,4-diphenyl 1,3-butadiene as a matrix. Electron paramagnetic resonance (EPR) studies were performed at the EPR Facility of Arizona State University. Continuous wave EPR spectra were recorded using an ELEXSYS E580 CW X-band spectrometer (Bruker, Rheinstetten, Germany) equipped with a Model 900 EPL liquid helium cryostat. For the measurements of Gov-1, the magnetic field modulation frequency was 100 kHz, the amplitude was 1 mT, the microwave power was 0.25 mW, the microwave frequency was 9.44 GHz, the sweep time was 84 s, and the temperature was 4 K. The EPR spectrum was simulated using EasySpin (version 5.1.10), a computational package developed by Stoll and Schweiger (2006) and based on Matlab (The MathWorks, Massachusetts, USA). The model used for the EPR

chemical window of the solvent. These results are consistent with the electron-withdrawing nature of the 3fluorophenyl substituents and previous reports on Co(II) tetrakis(3-fluorophenyl)porphyrin (Behar et al. 1998, Dhanasekaran et al. 1999), a known homogeneous electrocatalyst for the reduction of CO<sub>2</sub>. Nuclear magnetic resonance, electron paramagnetic resonance, UV-Vis absorption, and Fourier transform infrared spectroscopies coupled with mass spectrometry confirm successful synthesis of the target compound and provide information on the magnetic, electronic, and vibronic properties of the complex. The unique electron configuration surrounding the nucleus of fluorine in molecules (on average it is surrounded by nine electrons) results in a wider range and higher sensitivity of the fluorine chemical shifts than those typically encountered with other elements. In this article, we describe an unprecedented upfield <sup>19</sup>F resonance ascribed to the unique connectivity of the reported structure and resulting close proximity of one of the 3fluorophenyl groups to the ring current of the covalently attached 4-vinylphenyl surface attachment group.

simulations considered a low-spin  $^{59}$ Co(II) ion (S =  $\frac{1}{2}$ , I = 7/2). The fitting parameters were the g-values  $(g_x, g_y, and$  $g_z$ ) and the line widths ( $\Delta B_x$ ,  $\Delta B_y$ , and  $\Delta B_z$ ). The fitting procedure was similar to the one previously described by Flores et al. (2007). Fourier transform infrared spectroscopy (FTIR) was performed using a Bruker Vertex 70. Spectra were collected using transmission mode with a 1 cm<sup>-1</sup> resolution, GloBar MIR source, a broadband KBr beam splitter, and a liquid nitrogen cooled MCT detector. Cyclic voltammetry measurements were performed with a Biologic potentiostat using a glassy carbon (3 mm diameter) disk, a platinum counter electrode, and a silver wire pseudo-reference electrode in a conventional threeelectrode cell at a scan rate of 500 mV s<sup>-1</sup> at room temperature under argon. Anhydrous n-butyronitrile (Aldrich) was used as the solvent for electrochemical measurements. The supporting electrolyte was 0.1 M tetrabutylammonium hexafluorophosphate. The potential of the pseudo reference electrode was determined using the ferrocenium/ferrocene redox couple as an internal standard with  $E_{1/2}$  taken as 0.48 Volts vs. Standard Calomel Reference electrode (V vs. SCE) (Gobi et al. 1998).

**Synthesis**: **2-bromo-5,10,15,20-tetrakis(3-fluorophenyl) porphyrin (2)**: 5,10,15,20-tetrakis(3-fluorophenyl) porphyrin (80 mg, 0.12 mmol) was dissolved in a mixture of dichloromethane and methanol (9/1, v/v, 20 mL) and the solution was stirred and heated to reflux. After 25 min, a solution of N-bromosuccinamide (23 mg, 1.28 mmol), dissolved in 20 mL of a mixture of dichloromethane and methanol (9/1, v/v), was added dropwise over 35 min to the refluxing mixture. The reaction was quenched with

acetone (10 mL), and the solvent evaporated at reduced pressure. The crude residue was purified by column chromatography on silica using a mixture of 3:2 hexanes and chloroform as eluent to give the desired product (45%).  $^1\mathrm{H}$  NMR (400 MHz, CDCl<sub>3</sub>):  $\delta-2.94$  (2H, s, NH), 7.47–7.57 (4H, m, ArH), 7.64–7.76 (4H, m, ArH), 7.78–8.01 (8H, m, ArH), 8.75–8.95 (7H, m, βH); UV-Vis (CH<sub>2</sub>Cl<sub>2</sub>) 419, 515, 548, 590, 645 nm; MALDI-TOF-MS m/z calcd. for  $C_{44}H_{25}\mathrm{Br}F_4N_4$  764.12 and 766.12 obsd. 763.83 and 765.89.

5,10,15,20-tetrakis(3-fluorophenyl)-2-(4-vinylphenyl) porphyrin (3): 4-vinylphenyl boronic acid (4-VPBA) (71 mg, 0.5 mmol), potassium carbonate (133 mg, 1 mmol) and tetrakis(triphenylphosphine)palladium(0) (11 mg, 0.01 mmol) were added to a solution containing 2-bromo-5,10,15,20-tetrakis(3-fluorophenyl)porphyrin (73 mg, 0.1 mmol) dissolved in toluene (25 mL) and under an argon atmosphere. The reaction was heated to reflux and the progress of the reaction was monitored via thin-layer chromatography. The reaction was stopped following consumption of the porphyrin starting material (4 h) and the mixture was washed with a saturated solution of aqueous sodium bicarbonate then a saturated solution of aqueous sodium chloride. The organic phase was dried over sodium sulfate, filtered, and the solvent evaporated at reduced pressure. The residue was purified by column chromatography on silica using a mixture of 1:1 dichloromethane and hexanes as the eluent to yield the desired product (58%). <sup>1</sup>H NMR (400 MHz, CDCl<sub>3</sub>): δ – 2.72 (2H, s, NH), 5.30 (1H, d, J = 12 Hz, CH), 5.78 (1H, d, J = 20 Hz, CH), 6.76 (1H, dd, J = 20 Hz, J = 12 Hz, CH)7.02 (1H, td, J = 8 Hz, J = 2 Hz, ArH), 7.20 (1H, q, ArH), 7.26 (2H, d, J = 8 Hz, ArH), 7.33(2H, d, J = 8 Hz, ArH), 7.44–7.62 (4H, m, ArH), 7.64–7.77 (4H, m, ArH), 7.90– 8.04 (6H, m, ArH), 8.69–8.90 (7H, m, βH); UV-Vis (CH<sub>2</sub>Cl<sub>2</sub>) 419, 516, 550, 591, 647 nm; MALDI-TOF-MS m/z calcd. for C<sub>52</sub>H<sub>32</sub>F<sub>4</sub>N<sub>4</sub> 788.26 obsd. 788.00.

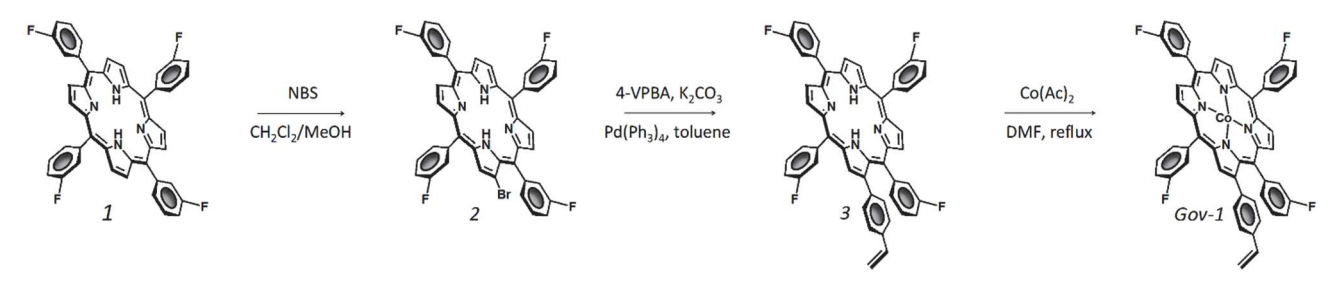
Cobalt(II) 5,10,15,20-tetrakis(3-fluorophenyl)-2-(4vinylphenyl)porphyrin (Gov-1): A mixture containing 5, 10,15,20-tetrakis(3-fluorophenyl)-2-(4-vinylphenyl) porphyrin (15 mg, 0.02 mmol) and cobalt(II) acetate (34 mg, 0.2 mmol) in dimethylformamide (23 mL) was stirred at reflux for 20 min. Upon cooling, the mixture was washed with a saturated solution of aqueous sodium bicarbonate then a saturated solution of aqueous sodium chloride and extracted with dichloromethane. The organic phase was dried over sodium sulfate, filtered, and the solvent evaporated at reduced pressure. The residue was purified by column chromatography on alumina using dichloromethane as eluent to give the desired product (98%). UV-Vis  $(CH_2Cl_2)$  412, 532 nm; MALDI-TOF-MS m/z calcd. for  $C_{52}H_{30}CoF_4N_4$  845.17 obsd. 844.96; EPR (CH<sub>2</sub>Cl<sub>2</sub>): ( $g_x =$  $2.081, g_v = 2.020, g_z = 1.966$ ). FTIR (KBr): 936; 955; 1,004; 1,077; 1,111; 1,151; 1,168; 1,185; 1,200; 1,264; 1,304;  $1,330; 1,347; 1,401; 1,430; 1,444; 1,480; 1,583; 1,610 \text{ cm}^{-1}$ .

Cobalt(II) 5,10,15,20-tetrakis(3-fluorophenyl)porphyrin (4): A mixture containing 5,10,15,20-tetrakis(3fluorophenyl) porphyrin (50 mg, 0.073 mmol) and cobalt(II) acetate (129 mg, 0.73 mmol) in dimethylformamide (70 mL) was stirred at reflux for 20 min. Upon cooling, the mixture was washed with a saturated solution of aqueous sodium bicarbonate then with a saturated solution of aqueous sodium chloride and extracted with dichloromethane. The organic phase was dried over sodium sulfate, filtered, and the solvent evaporated at reduced pressure. The residue was purified by column chromatography on alumina using dichloromethane as eluent. Recrystallization from dichloromethane/hexanes gave the target compound (96%). UV-Vis (CH<sub>2</sub>Cl<sub>2</sub>) 408, 527 nm; MALDI-TOF-MS m/z calcd. for C<sub>44</sub>H<sub>24</sub>CoF<sub>4</sub>N<sub>4</sub> 743.13 obsd. 742.79.

# **Results and discussion**

**Synthesis and characterization**: The synthetic strategy used to prepare the target compound, Gov-1, is depicted in Scheme 1. The starting material, 5,10,15,20-tetrakis(3-fluorophenyl)porphyrin (1), is synthesized according to previously reported literature procedures (Adler *et al.* 

1967, Tomkowicz *et al.* 2012). Bromination of *I* with N-bromosuccinamide (NBS) in a mixture of dichloromethane and methanol affords 2-bromo-5,10,15,20-tetrakis (3-fluorophenyl)porphyrin (2) in 45% yield. Successful monobromination at the beta position of the



Scheme 1. Synthetic scheme used to prepare cobalt(II) 5,10,15,20-tetrakis(3-fluorophenyl)-2-(4-vinylphenyl)porphyrin, Gov-1.

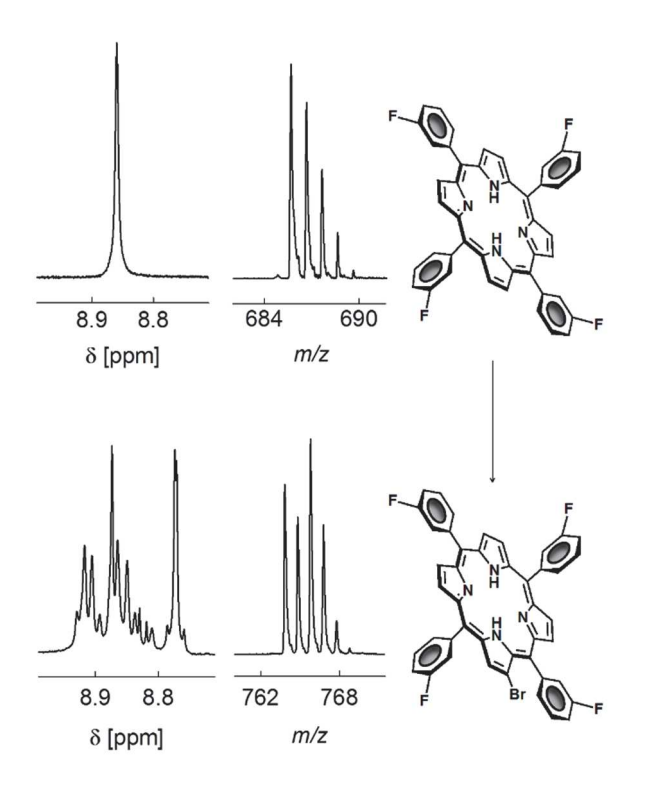


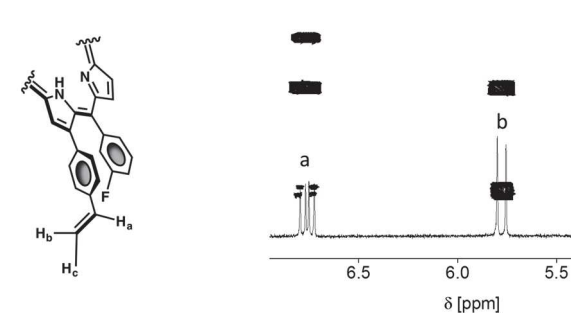
Fig. 1. <sup>1</sup>H NMR spectra showing the symmetry of  $\beta$ -pyrrolic protons of l (top left) and 2 (bottom left). MALDI-TOF MS data showing the isotopic distribution patterns of l (top center) and 2 (bottom center). Corresponding molecular structures of l (top right) and l (bottom right).

macrocycle is confirmed by NMR spectroscopy and MALDI-TOF mass spectrometry. In particular, the β-pyrrolic proton resonances in the  $^1$ H NMR spectrum of 2 are observed as a broad multiplet signal between 8.75–8.95 ppm that integrates to 7, consistent with the chemically and magnetically nonequivalent environments of the β-pyrrolic protons following the bromination reaction. This is in stark contrast to the starting compound I, where the fourfold symmetry of the macrocycle results in a single β-proton resonance that integrates to 8 and is centered at 8.86 ppm (Fig. 1). As anticipated for the unique isotopic

distribution associated with bromine-containing compounds, mass analysis of 2 reveals two isotope clusters with near equal intensities and mass-to-charge ratios consistent with compound 2 (see experimental section). In comparison with the absorption spectrum of 1, a 3 nm bathochromic shift is observed for the Soret absorption maximum as well as all four Q-bands, and the transition at 548 nm is diminished in relative intensity with respect to the other three Q-band transitions.

In the next synthetic step, a Suzuki cross-coupling reaction between 2 and 4-vinylphenyl boronic acid is used to prepare 5,10,15,20-tetrakis(3-fluorophenyl)-2-(4-vinylphenyl)porphyrin (3) with 58% yield. Confirmation of the molecular connectivity of 3 includes, but is not limited to, <sup>1</sup>H, <sup>13</sup>C, and <sup>19</sup>F NMR spectroscopy. The <sup>1</sup>H NMR spectrum of 3 shows the characteristic splitting pattern in the region of 5.11-6.90 ppm associated with the resonances of the vinylic protons and consistent with their assignments. The proton NMR spectrum of this region is shown in Fig. 2 along with the overlaid 2-dimensional gradient correlation spectroscopy (gCOSY) spectrum showing the cross-peak patterns assigned to trans- and cisvicinal coupling between the doublet of doublets ( $J=20 \,\mathrm{Hz}$ , J = 12 Hz) proton signal H<sub>a</sub> at 6.76 ppm and the signals assigned to the pair of geminal protons H<sub>b</sub> and H<sub>c</sub> appearing as doublets (J = 20 Hz and J = 12 Hz) at 5.78 ppm and 5.30 ppm, respectively. In the <sup>13</sup>C NMR spectrum of 3 a signal at 204.37 ppm is assigned to the deshielded carbons that are directly bound to fluorine. Finally, unlike the single triplet observed at −116.40 ppm in the <sup>19</sup>F spectrum of *I*, arising from the homotopic stereochemical relationship of the four fluoro groups and coupling to neighboring protons, the <sup>19</sup>F NMR spectrum of 3 confirms the presence of nonequivalent fluorine signals, including a relatively upfield triplet at -117.86 ppm. The upfield shift of this resonance is ascribed to the operation of a unique through space phenyl ring current effect induced by the nearby 4-vinylphenyl moiety.

In the final synthetic step, the target compound is prepared by treating porphyrin 3 with cobalt(II) acetate in a refluxing solution of dimethylformamide, yielding



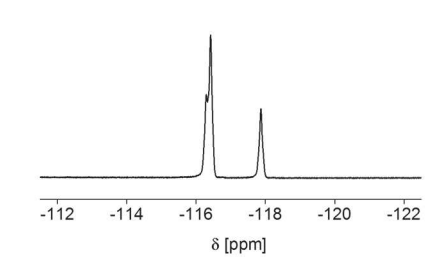


Fig. 2. Molecular structural fragment of compound 3 depicting a conformation in which the fluorine of a 3-fluorophenyl group is exposed to the ring current of the nearby 4-vinylphenyl moiety (left); <sup>1</sup>H NMR spectrum showing the vinylic proton region of 3 and the overlaid gCOSY spectrum (center); <sup>19</sup>F NMR of compound 3 showing the anisochronous resonances of the fluoro groups, including a significantly upfield resonance centered at -117.86 ppm (right).

5.0

cobalt(II) 5,10,15,20-tetrakis(3-fluorophenyl)-2-(4-vinylphenyl)porphyrin, Gov-1, with 98% yield, following purification via column chromatography. Successful insertion of cobalt into the tetrapyrrolic macrocycle of 3 is confirmed by the electronic absorption (UV-Vis) spectrum of the target molecule collected in dichloromethane. The absorbance spectrum of Gov-1 shows two intense bands with one component associated with the Soret-band transition at 412 nm and another for a Q-band transition appearing at 532 nm. This result is consistent with the approximate D<sub>4h</sub> symmetry of the macrocycle following the metal insertion. Conversely the Q-band transitions of the free-base porphyrins appear as four absorption bands due to the reduced symmetry. For the target compound, there is also a ≈5 nm bathochromic offset of the Soret– and Q- band transitions as compared to those observed in the absorption spectrum of cobalt(II) 5,10,15,20-tetrakis(3fluorophenyl) porphyrin (4), a model porphyrin compound that does not contain the 4-vinylphenyl functional group. The conversion of 3 into Gov-1 was also confirmed by FTIR spectroscopy; in particular, the transmission spectrum of Gov-1 does not contain the peak at 980 cm<sup>-1</sup> associated with pyrrolic in-plane N-H bending vibration of the free-base fluorinated porphyrin (3) (Alben et al. 1973). Instead, a new feature appears at  $\approx 1004$  cm<sup>-1</sup> that is associated with an in-plane cobalt porphyrin deformation (Boucher and Katz 1967, Kincaid and Nakamoto 1975). The FTIR transmission spectrum of Gov-1 also includes

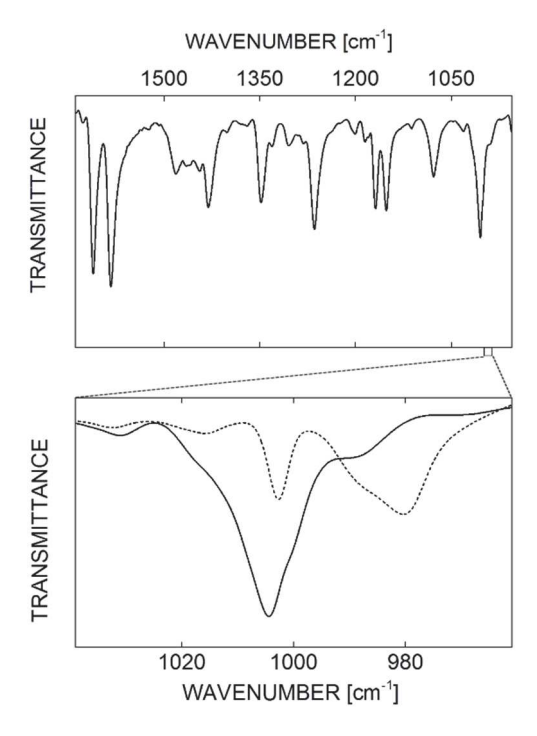


Fig. 3. FTIR transmittance spectrum of Gov-1 collected in KBr (top) and an expanded plot of the 961–1,039 cm<sup>-1</sup> region (bottom), showing the transmittance spectra of Gov-1 (solid) as well as the free-base precursor 3 (dash).

vibrational features assigned to  $C_{\beta}$ –H,  $C_{\alpha}$ – $C_{\beta}$  (1,078–1,111 cm<sup>-1</sup>),  $C_m-C_{ph}$  (1,265–1,303 cm<sup>-1</sup>),  $C_\alpha-N$  (1,347 cm<sup>-1</sup>),  $C_{\beta}=C_{\beta}$ ,  $C=C_{ph}$  (1,377–1,480 cm<sup>-1</sup>), and C-F (1,133–1,178, 1,554-1,627 cm<sup>-1</sup>) modes (Nguyen et al. 1999, Sun et al. 2003, Słota et al. 2011) (Fig. 3). The electronic structure of Gov-1 was also investigated using X-band (9.44 GHz) electron paramagnetic resonance (EPR) spectroscopy at 4 K (Fig. 4). The observed spectral features are consistent with a  $S = \frac{1}{2}$  spin system. To obtain the EPR parameters, the respective spin Hamiltonian was fit to the data (Fig. 4, bottom). The EPR spectrum of Gov-1 is well fit considering a low-spin  $^{59}$ Co(II) center (d<sup>7</sup>,  $S_{Co} = \frac{1}{2}$ ,  $I_{Co} =$ 7/2) with anisotropic g-values ( $g_x = 2.081$ ,  $g_y = 2.020$ ,  $g_z =$ 1.966) and non-resolved hyperfine coupling interactions between the magnetic moment of the unpaired electron and the magnetic moment of the <sup>59</sup>Co nucleus. Finally, mass analysis of Gov-1 shows a single isotope cluster and massto-charge ratio consistent with the target compound (see experimental section).

Electrochemical studies: The electrochemical properties of Gov-1 were studied via cyclic voltammetry in an argon sparged solution of 0.1 M tetrabutylammonium hexafluorophosphate in n-butyronitrile using a glassy carbon working electrode, a platinum counter electrode, and a silver wire pseudo reference with ferrocene as an internal standard (Fig. 5). Under these conditions, the voltammogram of Gov-1 shows three well defined redox features within the potential window + 0.98 to -2.22 V vs. SCE that for simplicity are assigned to metal-based redox processes. However, distinguishing ligand-based reductions from those that are metal-centered can be difficult and reductive processes of cobalt porphyrins have been ascribed to both innocent and non-innocent ligand chemistry (Kadish and Caemelbecke 2003, Sun et al. 2003, Lyaskovskyy and Bruin 2012, Luca and Crabtree 2013). This situation is of particular interest in connection with catalysis of multielectron redox processes by earth abundant metals where one-electron redox-state changes are often preferred. Assignments of the redox couples measured for Gov-1,

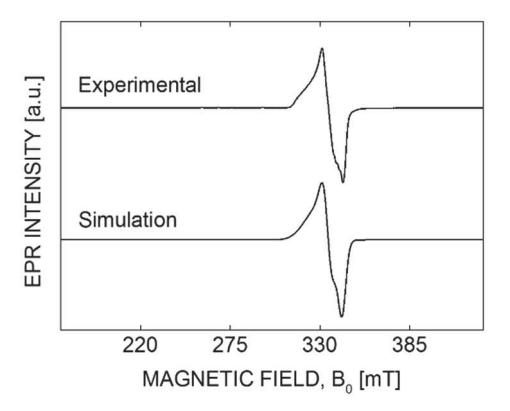


Fig. 4. Experimental (*top*) and simulated (*bottom*) X-band (9.44 GHz) EPR spectra of Gov-1 collected at 4 K in dichloromethane.

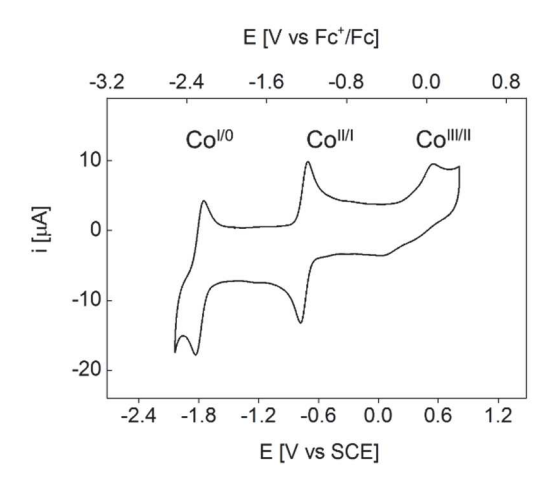


Fig. 5. Cyclic voltammogram of Gov-1 recorded in 0.1 M tetrabutylammonium hexafluorophosphate in n-butyronitrile under argon using a glassy carbon working electrode and a scan rate of  $500 \text{ mV s}^{-1}$ .

their midpoint potentials (<sup>n</sup>E<sub>1/2</sub>), and associated peak-topeak separations ( $\Delta E_p$ ) are listed in Table 1. The most oxidative feature, at  $E_{1/2}$  = + 0.29 V vs. SCE, is ascribed to the Co<sup>III</sup>/Co<sup>II</sup> couple, a quasi-reversible process with a relatively large peak-to-peak separation ( $\Delta E_p = 379 \text{ mV}$ ) due to sluggish electron transfer during the oxidation of low spin Co<sup>II</sup> ion and a slow self-exchange electron transfer rate (Chapman and Fleischer 1982, Sun et al. 2003). The Co<sup>II</sup>/Co<sup>I</sup> redox couple is assigned to the chemically reversible process occurring at  $E_{1/2} = -0.75 \text{ V}$ vs. SCE with a peak-to-peak separation of 72 mV and the Co<sup>I</sup>/Co<sup>0</sup> redox couple is assigned to the most reducing feature at  $E_{1/2} = -1.79$  V vs. SCE with a peak-to-peak separation of 77 mV. In comparison with cobalt(II) 5, 10,15,20-tetrakis(4-methylphenyl)-2-(4-vinylphenyl) porphyrin, the complex reported here allows access to the Co<sup>II</sup>/Co<sup>I</sup> and Co<sup>I</sup>/Co<sup>0</sup> relays at significantly less negative applied bias potentials. Likewise, these values are consistent with reports on the electrochemistry of

## References

Adler A.D., Longo F.R., Finarelli J.D. *et al.*: A simplified synthesis for meso-tetraphenylporphyrin. – J. Org. Chem. **32**: 476, 1966.

Alben J.O., Choi S.S., Adler A.D. et al.: Infrared spectroscopy of porphyrins. – Ann. NY Acad. Sci. 206: 278-295, 1973.

Bard A.J., Fox M.A.: Artificial photosynthesis: solar splitting of water to hydrogen and oxygen. – Acc. Chem. Res. 28: 141-145, 1995.

Behar D., Dhanasekaran T., Neta P *et al.*: Cobalt porphyrin catalyzed reduction of CO<sub>2</sub> radiation chemical, photochemical, and electrochemical studies. – J. Phys. Chem. A **102**: 2870-2877, 1998.

Beiler A.M., Khusnutdinova D., Jacob S.I. *et al.*: Solar hydrogen production using molecular catalysts immobilized on gallium phosphide (111)A and (111)B polymer – modified photocathodes. – ACS Appl. Mater. Interfaces **8**: 10038-10047, 2016a.

Table 1. Midpoint potentials for the reduction, <sup>nl</sup>E, and oxidation, <sup>nl</sup>E, of Gov-1. The peak-to-peak separation (mV) of the redox processes is listed in parentheses.

Compound	<sup>n</sup> E <sub>1/2</sub> potential (V vs <sup>II</sup> E (Co <sup>I/0</sup> or P/P <sup>-</sup> )	s. SCE) (ΔE <sub>p</sub> [m <sup>v</sup> <sup>I</sup> E (Co <sup>II/I</sup> )	V]) iE (Co <sup>III/II</sup> )
Gov-1	-1.79 (77)	-0.75 (72)	+0.29 (379)

cobalt(II) 5,10,15,20- tetrakis(3-fluorophenyl)porphyrin, a known homogeneous electrocatalyst for the reduction of CO<sub>2</sub>. Thus, installment of the 4-vinylphenyl moiety does not deactivate the ability of the fluorinated porphyrin complex to access the Co<sup>1</sup> and Co<sup>0</sup> states at relatively low (*i.e.* less negative) potentials.

**Conclusion**: A novel synthetic methodology to prepare a cobalt(II) tetrakis(3-fluorophenyl)porphyrin with a built-in 4-vinylphenyl surface attachment moiety is reported. Spectroscopic characterization, including: <sup>1</sup>H NMR, <sup>13</sup>C NMR, <sup>19</sup>F NMR, UV-Vis, FTIR, and EPR, as well as MALDI-TOF mass spectrometry confirms the molecular structure of the target molecule. Electrochemical studies reveal the meso 3-fluorophenyl substituents allow the complex to deliver relatively low potential Co<sup>I</sup> and Co<sup>0</sup> species as compared to a previously reported nonfluorinated analog. In this report, the complex is abbreviated as Gov-1 in recognition of Govindjee for his pioneering investigations in the role of fluorine as a promoter of novel protein-substrate interactions and the inspirational role he continues to have in encouraging young investigators in the areas of natural and artificial photosynthesis (Govindjee 2002, 2007, 2009, 2010; Govindiee and Telfer 2007, Govindiee et al. 2007, 2011, Moore et al. 2012b, Rappaport et al. 2015). We look forward to reporting the surface attachment chemistry and photoelectrochemical properties of this complex in a future report.

Beiler A.M., Khusnutdinova D., Jacob S.I. *et al.*: Chemistry at the interface: polymer-functionalized GaP semiconductors for solar hydrogen production. – Ind. Eng. Chem. Res. **55**: 5306-5314, 2016b.

Beiler A.M., Khusnutdinova D., Wadsworth B.L. *et al.*: Cobalt porphyrin-polypyridyl surface coatings for photoelectrosynthetic hydrogen production. – Inorg. Chem. **56**: 12178-12185, 2017.

Berben L.A., Peters J.C.: Hydrogen evolution by cobalt tetraimine catalysts adsorbed on electrode surfaces. – Chem. Commun. **46**: 398-400, 2010.

Boucher L.J., Katz J.J.: The infared spectra of metalloporphyrins (4000 – 160 [cm<sup>-1</sup>]). – J. Am. Chem. Soc. **89**: 1340-1345, 1967. Blankenship R.E., Tiede D.M., Barber J. *et al.*: Comparing photosynthetic and photovoltaic efficiencies and recognizing the potential for improvement. – Science **332**: 805-809, 2011.

- Cedeno D., Krawicz A., Doak P. *et al.*: Using molecular design to control the performance of hydrogen producing polymer-brush-modified photocathodes. J. Phys. Chem. Lett. **5**: 3222-3226, 2014.
- Cedeno D., Krawicz A., Moore G.F.: Hybrid photocathodes for solar fuel production: coupling molecular fuel-production catalysts with solid-state light harvesting and conversion technologies. Interface Focus 5: 20140085, 2015.
- Chambers R.D.: Fluorine in Organic Chemistry. Pp. 384. Blackwell Publishing Ltd. Oxford 2004.
- Chapman R.D., Fleischer E.B.: Direct measurement of electron self-exchange rates of cobalt porphyrins. 1. Outer-sphere exchange. J. Am. Chem. Soc. **104**: 1575-1582, 1982.
- Cicero R.L., Linford M.R., Chidsey C.E.D.: Photoreactivity of unsaturated compounds with hydrogen-terminated silicon (111). Langmuir **16**: 5688-5695, 2000.
- Dalvit C., Vulpetti A.: Fluorine protein interactions and <sup>19</sup>F NMR isotopic chemical shifts: an empirical correlation with implication for drug design. Chem. Med. Chem. **6**: 104-114, 2011.
- Dhanasekaran T., Grodkowski J., Neta P. *et al.*: p-terphenylsensitized photoreduction of CO<sub>2</sub> with cobalt and iron porphyrins. Interaction between CO and reduced metalloporphyrins. J. Phys. Chem. A **103**: 7742-7748, 1999.
- Faunce T.A., Lubitz W., Rutherford A.W. et al.: Energy and environment policy case for a global project on artificial photosynthesis. – Energy Environ. Sci. 6: 695-698, 2013a.
- Faunce T.A., Styring S., Wasiełewski M.R. *et al.*: Artificial photosynthesis as a frontier technology for energy sustainability. Energy Environ. Sci. 6: 1074-1076, 2013b.
- Flores M., Isaacson R., Abresch E. *et al.*: Protein-cofactor interactions in bacterial reaction centers from *Rhodobacter sphaeroides* R-26: II. Geometry of the hydrogen bonds to the primary quinone Qa. by <sup>1</sup>H and <sup>2</sup>H ENDOR spectroscopy. Biophys. J. **92**: 671-682, 2007.
- Gerig J.T.: Fluorine magnetic resonance in biochemistry. In: Berliner L.J., Reuben J. (ed.): Biological Magnetic Resonance (A Series of Contemporary Topics and Reviews), Vol. 1. Pp. 139-203, Springer, New York 1978.
- Gobi K.V., Tokuda K., Ohsaka T.: Electrochemical and spectroscopic studies on nickel(II/III) complexes with novel 14membered hexaaza macrocycle functionalized with propenyl groups. – Electrochim. Acta 43: 1013-1022, 1998.
- Govindjee: Celebrating Andrew Alm Benson's 93<sup>rd</sup> birthday. Photosynth. Res. **105**: 201-208, 2010.
- Govindjee: Young research investigators honored at the 2008 and 2009 Gordon research conferences on photosynthesis: ambiance and a personal perspective. Photosynth. Res. **102**: 1-6, 2009.
- Govindjee, Ananyev G.M., Savikhin S.: Young research investigators honored at the 2011 Gordon research conference on photosynthesis: ambiance and a perspective. Photosynth. Res. **110**: 143-149, 2011.
- Govindjee, Rutherford A.W., Britt R.D.: Four young research investigators were honored at the 2006 Gordon research conference on photosynthesis. Photosynth. Res. **92**: 137-138, 2007.
- Govindjee, Šesták Z., Peters W.R.: The early history of "Photosynthetica", "Photosynthesis Research", and their publishers. Photosynthetica **40**: 1-11, 2002.
- Govindjee, Telfer A.: Six young research investigators were honored at an international conference in Russia. Photosynth. Res. **92**: 139-141, 2007.

- Hou H.J.M., Najafpour M.M., Moore G.F. *et al.*: Photosynthesis: Structures, Mechanisms, and Applications. Pp. 321-358. Springer, New York 2017.
- Kadish K.M., Caemelbecke E.V.: Electrochemistry of porphyrins and related macrocycles. – J. Solid State Electrochem. 7: 254-258. 2003.
- Khusnutdinova D., Beiler A.M., Wadsworth B.L. *et al.*: Metalloporphyrin-modified semiconductor for solar fuel production. Chem. Sci. **8**: 253-259, 2017.
- Kim C.-Y., Chang J.S., Doyon J.B. *et al.*: Contribution of fluorine to protein ligand affinity in the binding of fluoroaromatic inhibitors to carbonic anhydrase II. J. Am. Chem. Soc. **122**: 12125-12134, 2000.
- Kincaid J., Nakamoto K.: Vibrational spectra of transition metal complexes of tetraphenylporphine. – J. Inorg. Nucl. Chem. 37: 85-89, 1975.
- Li B., Franking R., Landis E.C. *et al.*: Photochemical grafting and patterning of biomolecular layers onto TiO<sub>2</sub> thin films. ACS Appl. Mater. Interfaces. 1: 1013-1022, 2009.
- Luca O.R., Crabtree R.H.: Redox-active ligands in catalysis. Chem. Soc. Rev. **42**: 1440-1459, 2013.
- Lyaskovskyy V., de Bruin B.: Redox non-innocent ligands: versatile new tools to control catalytic reactions. ACS Catal. 2: 270-279, 2012.
- Maher A.G., Passard G., Dogutan D.K. *et al.*: Hydrogen evolution catalysis by a sparsely substituted cobalt chlorin. ACS Catal. 7: 3597-3606, 2017.
- Moore G.F.: Concluding remarks and future perspectives: looking back and moving forward. Pp. 407-414. Springer, New York 2017.
- Moore G.F., Ananyev G.M., Govindjee: Young research investigators honored at the 2012 Gordon Research Conference on Photosynthesis Photosynth. Res. **114**: 137-142, 2012a.
- Moore G.F., Hambourger M., Gervaldo M. *et al.*: A bioinspired construct that mimics the proton coupled electron transfer between P680\*+ and the Tyrz-His 190 pair of photosystem II. J. Am. Chem. Soc. **130**: 10466-10467, 2008.
- Moore G.F., Konezny S.J., Song H. *et al.*: Bioinspired high-potential porphyrin photoanodes. J. Phys. Chem. C **116**: 4892-4902, 2012b.
- Moore G.F., Sharp I.D.: A noble-metal-free hydrogen evolution catalyst grafted to visible light-absorbing semiconductors. J. Phys. Chem. Lett. **4**: 568-572, 2013.
- Najafpour M.M., Shen J-R., Barber J. *et al.*: Running on sun. Chem. World **November**: 43, 2012.
- Nguyen K., Day P.N., Pachter R.: Effects of halogenation on the ionized and excited states of free-base and zinc porphyrins. J. Chem. Phys. **110**: 9135-9144, 1999.
- O'Hagan D., Rzepa H. S.: Some influences of fluorine in bioorganic chemistry. Chem. Commun. 7: 645-652, 1997.
- Rappaport F., Malnoë A., Govindjee: Gordon research conference on photosynthesis: from evolution of fundamental mechanisms to radical re-engineering. Photosynth. Res. 123: 213-223, 2015.
- Richards D., Zemlyanov D., Ivanisevic A.: Assessment of the passivation capabilities of two different covalent chemical modifications on GaP(100). Langmuir 26: 8141-8146, 2010.
- Rose M.J., Gray H.B., Winkler J.R.: Hydrogen generation catalyzed by fluorinated diglyoxime-iron complexes at low overpotentials. J. Am. Chem. Soc. 134: 8310-8313, 2012.
- Rosenthal J., Luckett T.D., Hodgkiss J.M. *et al.*: Photocatalytic oxidation of hydrocarbons by a bis-iron(III)- $\mu$ -oxo pacman porphyrin using O<sub>2</sub> and visible light. J. Am. Chem. Soc. **128**:

- 6546-6547, 2006.
- Seifert M., Koch A.H.R., Deubel F. *et al.*: Functional polymer brushes on hydrogenated graphene. Chem. Mater. **25**: 466-470, 2013.
- Słota R., Broda M.A., Dyrda G. et al.: Structural and molecular characterization of meso-substituted zinc porphyrins: a DFT supported study. – Molecules 16: 9957-9971, 2011.
- Steenackers M., Gigler A.M., Zhang N. *et al.*: Polymer brushes on graphene. J. Am. Chem. Soc. **133**: 10490-10498, 2011.
- Stoll, S., Schweiger, A.: EasySpin, a comprehensive software package for spectral simulation and analysis in EPR. J. Magn. Reson. 178: 42-55, 2006.
- Sun H., Smirnov V., DiMagno S.G.: Slow electron transfer rates for fluorinated cobalt porphyrins: electronic and conformational factors modulating metalloporphyrin ET. Inorg. Chem. **42**: 6032-6040, 2003.
- Sykes B.D., Hull W.E., Snyder G.H.: Experimental evidence for role of cross-relaxation in proton nuclear magnetic resonance spin lattice relaxation time measurements in proteins. Biophys. J. 21: 137-146, 1978.

- Tierno M.E., Mead D., Asato A.E. *et al.*: 14-fluorobacteriorhodopsin and other fluorinated and 14-substituted analogues. An extra, unusually red-shifted pigment formed during dark adaptation. Biochemistry **29**: 5948-5953, 1990.
- Toi H., Homma M., Suzuki A. *et al.*: Paramagnetic <sup>19</sup>F N.M.R. spectra of iron(III) porphyrins substituted with CF<sub>3</sub> groups and reconstituted myoglobin. J. Chem. Soc. Chem. Comm. **24**: 1791-1792, 1985.
- Tomkowicz Z., Rams M., Bałanda M. *et al.*: Slow magnetic relaxations in manganese(III) tetra(*meta-*fluorophenyl)-porphyrin-tetracyanoethenide. Composition with the relative single chain magnet *ortho* compound. Inorg. Chem. **51**: 9983-9994, 2012.
- Wadsworth B.L., Beiler A.M., Khusnutdinova D. *et al.*: Electrocatalytic and optical properties of cobaloxime catalysts immobilized at a surface-grafted polymer interface. ACS Catal. **6**: 8048-8057, 2016.
- Yolder N.C., Kumar K.: Fluorinated amino acids in protein design and engineering. – Chem. Soc. Rev. 31: 335-341, 2002.